RNF43 and PWWP2B inhibit cancer cell proliferation and are predictive or prognostic biomarker for FDA-approved drugs in patients with advanced gastric cancer

Sung-Hwa Sohn
Hallym University Sacred Heart Hospital
Hee Jung Sul
Hallym University Sacred Heart Hospital
Bohyun Kim
Hallym University Sacred Heart Hospital
Hyeong Su Kim
Hallym University Sacred Heart Hospital
Hyun Lim
Hallym University Sacred Heart Hospital
Ho Suk Kang
Hallym University Sacred Heart Hospital
Jae Seung Soh
Hallym University Sacred Heart Hospital
Kab Choong Kim
Hallym University kangnam scared hospital
Ji Woong Cho
hallym university kangnam scared hospital
Jinwon Seo
Hallym University College of Medicine
Youngho Koh
Ilsong Institute of Life Science
Dae Young Zang (fhdzang@gmail.com)
Hallym University Sacred Heart Hospital https://orcid.org/0000-0002-2602-7848

Primary research

Keywords: anti-cancer drugs; gastric cancer; PWWP2B; RNF43; docetaxel trihydrate; pelitinib; uprosertib

Posted Date: May 6th, 2020

DOI: https://doi.org/10.21203/rs.3.rs-25882/v1

Abstract

Background

The characterization of gastric cancer has necessitated the development of new therapeutics as well as the identification of prognostic markers to predict the response to novel drugs. In our study, we have performed RNA sequencing analysis on gastric cancer tissues that decreased levels of RNF43 and PWWP2B were significantly associated with recurrence (11/11, 100%, $P < 0.001$). Therefore, we investigated the screening of 1,449 FDA-approved drugs in HAP1, HAP1 RNF43 KO and HAP1 PWWP2B KO cells.

Methods

We demonstrated that RNF43 KO and PWWP2B KO cells showed significantly increased proliferation and migration abilities. Next, we investigated the inhibitory effects of 1,449 drugs in HAP1, HAP1 RNF43 KO and HAP1 PWWP2B KO cells.

Results

Among these FDA-approved drugs, three drugs (docetaxel trihydrate, pelitinib and uprosertib) showed strong inhibitory effects in RNF43 KO cells and PWWP2B KO cells. In RNF43 and PWWP2B down-regulated MKN45 xenograft model, tumor volumes were significantly reduced in the docetaxel trihydrate, uprosertib or pelitinib-treated group. Our data demonstrated that RNF43 and PWWP2B are a biomarker that predict recurrence of gastric cancer.

Conclusion

Our findings suggest that docetaxel trihydrate, uprosertib and pelitinib could be used as novel therapeutic agents for the prevention and treatment of gastric cancer with an aberrant decrease in RNF43 and PWWP2B expression.

Background

Gastric cancer is the fifth most common cancer and third leading cause of cancer deaths worldwide, especially in Eastern Europe, South America, and Eastern Asia (mainly China, Japan, and Korea) [1–3]. However, gastric cancer incidence has decreased markedly in Asian countries in recent years [4]. In South Korea, despite a decline in incidence, it is the second most common cancer [5]. In addition, unsatisfactory treatment outcomes are caused by differences of the molecular basis and intrinsic biological factors [6, 7]. In an effort to overcome this problem, and to develop and identify new drug candidates, determining tumor characteristics and treatment parameters is important in Eastern Asia. Furthermore, the majority of

cancers are loss-of-function events that defy standard inhibitor-based drug screening strategies. One strategy for overcoming the loss of function is to perform high-throughput screening using target gene knockout (KO) cell lines.

RNF43 encodes a transmembrane ubiquitin E3 ligase and is a tumor-suppressing gene that suppresses the Wnt/β-catenin signaling pathway, which is often the cause of cancer [8–10]. Loss-of-function mutations in RNF43 promote reinforced cell proliferation and result in neoplastic transformation [11]. Recent studies revealed that RNF43 suppresses proliferation and induces apoptosis in gastric carcinoma cells [8, 12].

In this study, we applied an RNA sequencing (RNA-seq) approach to identify RNF43 (i.e., verify a known marker) and PWWP2B (i.e., explore a novel marker) genes differentially expressed in gastric cancer and adjacent normal tissues from 34 patients. To identify Food and Drug Administration (FDA)-approved drugs that selectively target cancer cells with inactivated RNF43 and PWWP2B genes, we performed a high-throughput screening of 1,449 drugs in HAP1, HAP1 RNF43 KO, HAP1 PWWP2B KO, and SNU620 cells. This study was conducted to identify anti-cancer drugs in gastric cancer with an aberrant decrease in RNF43 and PWWP2B expression.

Methods

Study subjects and gastric tissue specimen collection

Gastric cancer and adjacent normal tissues obtained from 34 patients who underwent initial surgery at Hallym University Sacred Heart Hospital from March 2014 to July 2015, were selected as the discovery cohort for RNA-seq. All cases were prospectively followed up for at least 3 year. Table 1 summarizes the discovery sets. This study was approved by the Ethics Committee of Hallym University Sacred Heart Hospital (2015-I078). Written informed consent was obtained from all of the participants.

RNA-seq and differentially expressed gene (DEG), single-nucleotide polymorphism (SNP), and insertions/deletions (indels) analyses

Gastric cancer and adjacent normal tissues from 34 patients were subjected to RNA-seq. Total RNA was extracted with TRIzol Reagent. Beads containing oligo (dT) were used to isolate poly(A) mRNA from total RNA. mRNA was fragmented, and first-strand cDNA was synthesized using random hexamer primers. Second-strand cDNA was synthesized using dNTPs, RNase H, and DNA polymerase I. Next, short double-stranded cDNA fragments were ligated to Illumina sequencing adaptors. DNA fragments were gel-purified and amplified by polymerase chain reaction (PCR). The amplified library was sequenced on an Illumina HiSeq 2500 sequencing machine. The raw reads were saved in the FASTQ format, and the dirty raw reads were removed before analyzing the data. Reads that could be uniquely mapped to a gene were used to calculate gene expression levels, which were measured based on the number of reads per kilobase of transcript per million mapped reads. We identified DEGs between paired tumor and normal samples and

considered $P \leq 0.001$ as significant. The comprehensive detection of SNPs and small indels followed the method described by Yoon et al. (2013)[13] and Lee et al (2014)[14], with slight modifications.

Cell lines and cell culture

The male and female human cell lines used in this study. HAP1, HAP1 RNF43 KO, and HAP1 PWWP2B KO cells (derived from 40year male chronic myelogenous leukemia) were obtained from Horizon. SNU620 (derived from 59year female gastric adenocarcinoma), MKN28 (derived from 37year male gastric tubular adenocarcinoma), MKN45 (derived from 62year female gastric adenocarcinoma), and KatoIII (derived from 57year male Signet ring cell gastric adenocarcinoma) cells were obtained from the Korean Cell Line Bank. The cells were grown and maintained under conditions of 100% humidity and 5% CO_2 at 37°C in Iscove's modified Dulbecco's medium (IMDM) or RPMI 1640 medium supplemented with 10% fetal bovine serum (FBS) and 1% streptomycin and penicillin (Invitrogen Life Technologies, Rockville, MD, USA). The cells were plated onto tissue culture flasks (T-75 cm^2) at a density of 1×10^7/mL in hormonally defined IMDM or RPMI 1640 medium as described previously. The medium was changed every 3 days until the cells reached 80–90% confluence, at which point they were used in the experiments.

Morphological evaluation

Microscopical studies of the HAP1, HAP1 RNF43 KO, and HAP1 PWWP2B KO cells were carried out with a Microscope. The magnification was 400 fold.

Cell size analysis

HAP1, HAP1 RNF43 KO, and HAP1 PWWP2B KO cells seeded onto 6-well plates at a density 5×10^4 cells per mL. Cell size was determined using a CytoFLEX flow cytometer (Beckman Coulter, Brea, CA, USA). The use of the flow cytometry parameters forward (FSC) and sideward (SSC) scatter of the cells give an indication on gene KO effects through the relative cell size.

Quantitative real-time PCR analysis

RNA was isolated from cells using TRIzol reagent (Invitrogen, Carlsbad, CA, USA) according to the manufacturer's instruments, and quantified on a NanoDrop ND-1000 device (Thermo Scientific, Wilmington, DE, USA). Complementary DNA (cDNA) was synthesized using the High Capacity cDNA Reverse Transcription Kit (Applied Biosystems, Foster City, CA, USA). Quantitative real-time (qRT) PCR was performed using Power SYBR Green PCR Master Mix on a LightCycler 96 instrument (Roche Applied Science, Indianapolis, IN, USA). The transcript levels of glyceraldehyde-3-phosphate dehydrogenase (GAPDH) were used for sample normalization. Primer sequences were as follows: RNF43 (FW 5'-CTG TCA CTG GCT AGC AAG G-3'; RW 5'-AGC TTC TCA GCG TCA TTA CC-3'), PWWP2B (RT2 qPCR Primer Assay, Qiagen, Inc., Valencia, CA, USA), and GAPDH (FW 5'-GAG TCA ACG GAT TTG GTC G-3'; RW 5'-TGG AAT CAT ATT GGA ACA TGT AAA C-3').

Immunohistochemical analysis

Immunohistochemical (IHC) analysis of RNF43 was performed. Tissue sections were treated with 3 % hydrogen peroxide, and nonspecific binding sites were blocked. The sections were incubated with anti-RNF43 antibodies (AP13204B, ABGENT, San Diego, CA, USA). An automatic immunostainer (BenchMark XT; Ventana Medical Systems, Inc, Tucson, AZ, USA) and UltraView Universial DAB detection kit (Ventana Medical Systems) were used for immunostaining.

Cell proliferation assay

The proliferation of HAP1, HAP1 RNF43 KO, and HAP1 PWWP2B KO cells was assessed using the MTT assay. Cells were cultured in 96-well plates (2×10^4/mL) for 0, 24, 48, and 72 h. MTT solution (5 mg/mL) was added at the end of incubation, which was continued for 4 h. The reaction was terminated by adding a detergent reagent. The absorbance was read at 570 nm using a microplate reader (Synergy 2 Multi-Mode Microplate Reader; BioTek, Winooski, VT, USA).

Colony forming assay

HAP1, HAP1 RNF43 KO, and HAP1 PWWP2B KO cells were diluted and seeded at a density of approximately 5,000 cells per well in 6-cm plates. After incubation for 7 days, colony formation and growth were visualized with crystal violet staining. After the wells were photographed, the dye was solubilized with methanol and the optical density was measured at 570 nm using a microplate reader.

Cell migration assay

HAP1, HAP1 RNF43 KO, and HAP1 PWWP2B KO cells were diluted and seeded at a density of approximately 1×10^5 cells per well in 6-cm or 24-well plates. After incubation for 1 day, a straight scratch was made on the cells using a P200 pipette tip. The cells were then washed with PBS and further cultured with or without docetaxel trihydrate, pelitinib, and uprosertib in IMDM. After incubation for 0, 48, and 72 h, the gap width of the scratch re-population was photographed and then compared with the initial gap size at 0 h.

High-throughput drug screening

An FDA-approved compound library of 1,448 drugs was purchased from Selleck Chemicals. INC280 was supplied from Novartis (Basel, Switzerland). HAP1, HAP1 RNF43 KO and HAP1 PWWP2B KO cells were seeded at a density of 2,000 or 3,000 cells per well in 384-well, clear-bottom culture plates with 20 μL IMDM or RPMI 1640 medium containing 10% FBS for 24 h. Then, 10 μM of FDA-approved drug was added to the wells, and the cells were incubated for an additional 48 h. Control cells were not exposed to drugs. On the day of the proliferation assay, the medium was removed, 20 μL of fresh medium was added to each well of the 384-well plates, followed by 5 μL of MTS solution (Cell Titer 96 Aqueous One Solution Cell Proliferation Assay Kit; Promega, Madison, WI, USA), and the plates were incubated at 37°C for 1 h in a humidified environment with 5% CO_2. The absorbance was read at 490 nm using a PerkinElmer (Waltham, MA, USA) EnVision luminescence microplate reader. Data were validated using the Z′ factor

analysis. The percentage inhibition was expressed as [viability level of test samples/viability level of control)] × 100.

Confirmatory growth inhibition assays

The half maximal inhibitory concentrations of the selected drugs of HAP1, HAP1 RNF43 KO and HAP1 PWWP2B KO cells were measured using the MTS assay for selected drugs at concentrations of 40, 20, 10, 5, 2.5, 1.25, 0.625, and 0.3125 μM for 48 h. On the day of the proliferation assay, medium was removed, and 100 μL of fresh medium was added to each well of 96-well plates, followed by 20 μL of MTS solution, and the plates were incubated at 37°C for 1 h in a humidified environment with 5% CO_2. The absorbance was read at 490 nm using a microplate reader (Synergy 2 Multi-Mode Microplate Readers; BioTek, Winooski, VT, USA). The IC_{50} values were determined after fitting growth inhibition curves to dose–response curves using GraphPad Prism software (GraphPad Software Inc., CA, USA).

Apoptosis analysis

HAP1, HAP1 RNF43 KO, HAP1 PWWP2B KO, SNU620, Kato III, MKN28, and MKN45 cells seeded onto 6-well plates at a density 5×10^4 cells per mL were treated with the respective IC50 values of docetaxel trihydrate, pelitinib, and uprosertib (Table 2). Cell death was determined using the Annexin V-APC/Propidium Iodide (PI) Apoptosis Detection Kit (Thermo Fisher Scientific, Rockford, IL, USA) on a CytoFLEX flow cytometer (Beckman Coulter, Brea, CA, USA). The percentages of intact and apoptotic cells were calculated using CytExpert software (Beckman Coulter).

In vivo tumor growth inhibition studies

All the experiments and animal handling procedures in this study were approved by the Animal Experimental Ethics Committee of the Asan Medical Center, Seoul, Korea. Six-week-old male BALB/c-nu/nu mice (Joongang Laboratory Animal Inc., Seoul, Korea) were housed in cages, and maintained at 23ºC with a 12-h light/dark cycle under specific pathogen free conditions. Each mouse was inoculated subcutaneously (s.c.) into the right flank with either 1×10^7 cells/mouse of human gastric cancer cell line MKN45. When the average s.c. tumor volume reached 100 mm^3, the mice were randomly divided into various treatment and control group (5 mice per group). Tumor size was measured twice every week with caliper (calculated volume = shortest $diameter^2$ x longest diameter/2). Body weight and tumor size were recorded twice every week. After three weeks, the mice were sacrificed.

Statistical analysis

The data were statistically analyzed using Prism 5 (GraphPad Software Inc.). All values are presented as means ± the standard error of the mean. Statistical significance was examined with the Mann–Whitney test or Fisher's exact test. A value of $P < 0.05$ was considered statistically significant.

Results

Baseline characteristics

A total of 34 subjects were enrolled in this study to gain insight into the molecular pathogenesis of gastric cancer in a Korean population. We searched for genetic alterations using RNA-seq in gastric cancer samples and their matched adjacent normal tissues. By comparing the transcriptome sequences of the cancer tissues with their matched normal tissues, we identified differentially expressed genes, including RNF43 and PWWP2B. The associations of RNF43 and PWWP2B expression with clinicopathological characteristics are shown in Table 1. The subjects included 19 males (55.9%) and 15 females (44.1%), with a median age of 68.6 years (range: 44–87 years). Eleven patients had recurrence. Low expression of RNF43 and PWWP2B (100%, $P < 0.001$) was significantly associated with recurrence (Table 1). We found RNF43 and PWWP2B mutations in 7 of 34 tumors and 6 of 34 tumors, respectively (Fig. 1a). In addition, 34 tumors carried germline RNF43 mutations. The IHC analysis of RNF43 showed not detect of RNF43 in gastric cancer tissue with low or high expression of RNF43 gene (Fig. 1b).

Cell proliferation and migration regulation by RNF43 and PWWP2B

In light microscopy we first investigated the cell size effect of RNF43 KO or PWWP2B KO compared to WT cells (Fig. 2a). The KO of RNF43 and PWWP2B show only visible influence on the cell size of PWWP2B KO cells. The morphological parameters of the FACS analysis shows only altered cell size in PWWP2B KO cells (Fig. 2a). The effects of RNF43 KO and PWWP2B KO on cell proliferation, we investigated cell proliferation using MTT and colony formation assays (Fig. 1b and 1c). RNF43 KO and PWWP2B KO increased the proliferation and colony formation of HAP1 cells. Especially, PWWP2B KO cell line formed colonies much larger than WT and RNF43 KO cells, suggesting that the PWWP2B KO might endow gastric cancer cells with accelerated tumorigenic capability. Then we investigated cell migration using the wound-healing assay. RNF43 KO and PWWP2B KO increased migration in HAP1 cells (Fig. 2d). These results suggest that the loss of RNF43 and PWWP2B may modulate cell migration.

FDA-approved drug library screen

To evaluate the effect of the 1,449 FDA-approved drugs on HAP1, HAP1 RNF43 KO and HAP1 PWWP2B KO cell viability, cells were treated with 10 μM of FDA-approved drugs for 48 h, and the inhibitory effect of the drugs was evaluated using the MTS assay. After 48 h, the cell viability of the drug-treated cells was lower than that of the untreated control cells, with 9 drugs resulting in cell viability less than 40% in HAP1 cells. The cells were treated with different concentrations of each drug for 48 h, and the optimal dose was determined by evaluating cell viability using MTS assays. Treatment with the nine drugs (aprepitant, docetaxel trihydrate, ethinyl estradiol, griseofulvin, INC280, pelitinib, pimobendan, tepotinib, and uprosertib) decreased cell viability in a dose-dependent manner ($n = 3$). The IC50 values of the nine drugs were determined using non-linear regression analysis (Table 2). Among these drugs, docetaxel trihydrate, pelitinib, and uprosertib showed the best inhibition rates.

Effects of three drugs on cell migration

To determine the inhibitory effects of docetaxel trihydrate, pelitinib, and uprosertib on HAP1, HAP1 RNF43 KO, and HAP1 PWWP2B KO cells, cell migration was examined by performing a wound healing assay with the respective IC50 values of the three drugs (Fig. 3a-c). The wound gaps in the cells treated with each of the three drugs were significantly wider than those of the untreated groups at 48 and 72 h. IC50 values of these drugs, pelitinib and uprosertib showed the best inhibitory effect.

Effects of three drugs on cell apoptosis

To evaluate the effects of docetaxel trihydrate, pelitinib, and uprosertib on cell death in HAP1, HAP1 RNF43 KO, HAP1 PWWP2B KO, SNU620, Kato III, MKN28, and MKN45 cells, apoptosis was examined by staining with annexin V-APC/PI followed by flow cytometry (Fig. 4-5). Cells were stained with annexin V-APC and PI, which assess early apoptosis and the rate of apoptosis in a cell population. Docetaxel trihydrate showed the best cell death rates in HAP1, RNF43 KO, PWWP2B KO, SNU620, and Kato III cells (Fig. 4-5). Pelitinib showed the best cell death rates in MKN45 cells (Fig. 5d). RNF43 and PWWP2B genes were weakly expressed in MKN45 cells compared with the other cell types (Additional file 1). The percentage of apoptotic cells was 10%, 15%, and 6% after exposure to docetaxel trihydrate, pelitinib, and uprosertib, respectively, while that of control cells was only 3% (Fig. 5). In contrast, these drugs were not effects MKN28 cells, which highly express PWWP2B (Fig. 5 and Additional file 1).

In vivo anti-tumor efficacy of three drugs in tumor xenografts

Prompted by the in vitro data supporting a potential anti-tumor activity of docetaxel trihydrate, pelitinib, and uprosertib, we examined the in vivo efficacy of 3 drugs on the growth of MKN45 xenograft models. As demonstrated in Fig. 6, mice bearing s.c. MKN45 tumors were treated with docetaxel trihydrate (blocking tubulin), pelitinib (blocking EGFR), and uprosertib (blocking AKT). The docetaxel trihydrate, pelitinib, and uprosertib could significantly inhibit tumor growth at 3 weeks with the inhibition rate 49%, 31%, and 27% in KMN45 xenografts, respectively. The docetaxel trihydrate and pelitinib were well tolerated as demonstrated by the weight gain of treatment groups over the treatment period (Fig. 6).

Discussion

Unsatisfactory treatment outcomes occur in Asian countries due to differences in the intrinsic biological factors and rate of diagnosis of gastric cancer between Western and Eastern countries, which represents a major impediment in this field [6, 7]. Therefore, in the present study, 1,449 FDA-approved drugs were screened according to the tumor characteristic status in Korea.

Aberrant regulation of Wnt/β-catenin signaling is observed in colon, ovarian, lung, prostate, liver, breast, and gastric cancers [12, 15–20]. Wnt/β-catenin signaling mediates the epithelial-to-mesenchymal transition in gastric cancer [21], a process whereby epithelial cells are converted into migratory and invasive cells [22, 23]. RNF43 is encoded by Wnt target genes, and the loss of expression of this E3 ligase has been predicted to result in hyper-responsiveness to endogenous Wnt signals [11]. *RNF43* is a tumor suppressor gene in mucinous ovarian cancers, mucinous pancreatic precancerous cysts, and gastric

cancer [8, 24–27]. The PWWP domain is an essential component of DNMT3B that promotes tumorigenesis and contributes to aberrant DNA methylation in carcinogenesis [28]. Using a gastric cancer cohort, we retrospectively evaluated the relationship between RNF43 and PWWP2B expression levels and clinical characteristics. We found that gastric cancer recurrence patients showed downregulated RNF43 and PWWP2B (100%). In addition, we found RNF43 and PWWP2B mutations in 7 and 6 of 34 gastric cancer patients, respectively. In addition, 34 gastric cancer patients carried germline RNF43 mutations. The RNF43 and PWWP2B genes are potential biomarkers candidates for patients with advanced gastric cancer. Therefore, we examined the action of RNF43 and PWWP2B in RNF43 KO and PWWP2B KO cell lines. Our results showed that the cellular capacity for proliferation and migration was markedly increased in RNF43 KO and PWWP2B KO cell lines compared with the wild type control. These data suggest that downregulation of RNF43 and PWWP2B might promote proliferation of gastric cancer cells and could be a condition for the conversion of normal gastric epithelial cells into cancerous cells.

Used simultaneously, cell- and target-based screening procedures might be the optimal methods for promoting cancer drug discovery. They can be used to screen large numbers of drugs to determine their therapeutic potential, and correlations between target genes and clinical characteristics. Therefore, in this study, 1,449 FDA-approved drugs were screened to determine whether they could be used as therapeutic agents for the treatment of gastric cancer using growth inhibition assays of HAP1, HAP1 RNF43 KO and HAP1 PWWP2B KO cells. Among the 1,449 FDA-approved drugs tested, nine (aprepitant, docetaxel trihydrate, ethinyl estradiol, griseofulvin, INC280, pelitinib, pimobendan, tepotinib, and uprosertib) showed high inhibitory activity; therefore, these drugs were selected for further study. Table 2 presents the IC50 values and effective doses of these drugs. Docetaxel trihydrate, pelitinib, and uprosertib, which showed the highest inhibition and apoptotic rates of the tested drugs, have been shown to have therapeutic utility. For example, AKT signaling is responsible for development of resistance in cancer to various chemotherapeutics drugs [29]. The downstream protein GSK3ß is major AKT substrate. Docetaxel trihydrate is used widely to treat recurrent or gastric cancer [30, 31]. Docetaxel treatment inhibit phosphorylation state of GSK3ß [32]. Pelitinib is used to treat lung cancer [33]. Pelitinib is also an inhibitor of epidermal growth factor receptor (EGFR), making it active against putative EGFR-dependent tumor types [34, 35]. In addition, Pelitinib inhibit EGF-induced activation of AKT and ERK1/2 in cancer cells [36]. Uprosertib is used in recurrent or persistent ovarian cancer, endometrial cancer, and melanoma [37, 38]. Uprosertib is a broad AKT inhibitor used not only for the treatment of gastric cancer, but also for AKT-dependent cancers [39]. It is well-known that active AKT phosphorylates Gsk3β on serine 9, thereby inactivating it [40]. Gsk3β inhibits Wnt/β-catenin signaling by inhibiting AKT in gastric cancer.

Conclusion

The results of this study indicate that RNF43 and PWWP2B are differentially expressed in gastric cancers compared with normal adjacent gastric mucosa. Furthermore, a correlation between low RNF43 and PWWP2B expression and tumor recurrence was seen. Docetaxel trihydrate, pelitinib, and uprosertib have significant inhibitory activity in cancers with low RNF43 and PWWP2B expression; therefore, further

studies are needed to elucidate their mechanisms of action should to aid in the discovery of new therapeutic agents for the treatment of gastric cancer.

Abbreviations

RNA-seq: RNA sequencing; FDA: Food and Drug Administration; DEG: differentially expressed gene; SNP: single-nucleotide polymorphism; indels:insertions/deletions; IMDM: Iscove's modified Dulbecco's medium; FBS: fetal bovine serum; IHC: Immunohistochemical; IC_{50}: :half maximal inhibitory concentration.

Declarations

Acknowledgements

Not applicable

Ethical approval and consent to participate

Ethical registry was obtained from the Institutional Review Board and Ethics Committee of Hallym University Sacred Heart Hospital prior to the beginning of the study under No. 2015-I078. Written, informed consent was obtained from all participants prior to their inclusion in this study.

Consent for publication

Not applicable.

Availability of data and materials

The datasets used and/or analyzed for the current study are available from the corresponding author on reasonable request.

Conflicts of interest: The authors have no conflict of interest to declare.

Funding: This research was supported by the National R&D Program for Cancer Control, Ministry of Health and Welfare (HA17C0054), the Ministry of Food and Drug Safety (awarded in 2018, 18183MFDS491) of Korea, and Hallym University Research Fund.

Author Contributions: SHS performed molecular experiments, analyzed data and drafted the article. HJS and BK performed molecular experiments. HSK and BH analyzed the clinicopathological results, HL, HSK, JSS, KCK, JWC, and JS material support, HK and YK critical revision of the manuscript for important intellectual content. DYZ study supervision, obtained funding, guided the analysis of data and edited the manuscript. All authors read and approved the final manuscript.

References

1. Peleteiro B, Severo M, La Vecchia C, Lunet N. Model-based patterns in stomach cancer mortality worldwide. Eur J Cancer Prev. 2014;23(6):524–31.
2. Peleteiro B, Barros S, Castro C, Ferro A, Morais S, Lunet N. Worldwide burden of gastric cancer in 2010 attributable to high sodium intake in 1990 and predicted attributable burden for 2030 based on exposures in 2010. Brit J Nutr. 2016;116(4):728–33.
3. Ferro A, Peleteiro B, Malvezzi M, Bosetti C, Bertuccio P, Levi F, Negri E, La Vecchia C, Lunet N. Worldwide trends in gastric cancer mortality (1980–2011), with predictions to 2015, and incidence by subtype. Eur J Cancer. 2014;50(7):1330–44.
4. Park MS, Yoon JY, Chung HS, Lee H, Park JC, Shin SK, Lee SK, Lee YC. Clinicopathologic Characteristics of Interval Gastric Cancer in Korea. Gut Liver. 2015;9(2):167–73.
5. Jung KW, Won YJ, Kong HJ, Oh CM, Lee DH, Lee JS. Cancer Statistics in Korea: Incidence, Mortality, Survival, and Prevalence in 2011. Cancer Res Treat. 2014;46(2):109–23.
6. Strong VE, Song KY, Park CH, Jacks LM, Gonen M, Shah M, Coit DG, Brennan MF. Comparison of gastric cancer survival following R0 resection in the United States and Korea using an internationally validated nomogram. Ann Surg. 2010;251(4):640–6.
7. Chahal NS, Lim TK, Jain P, Chambers JC, Kooner JS, Senior R. Ethnicity-related differences in left ventricular function, structure and geometry: a population study of UK Indian Asian and European white subjects. Heart. 2010;96(6):466–71.
8. Niu L, Qin HZ, Xi HQ, Wei B, Xia SY, Chen L. RNF43 Inhibits Cancer Cell Proliferation and Could be a Potential Prognostic Factor for Human Gastric Carcinoma. Cell Physiol Biochem. 2015;36(5):1835–46.
9. de Lau W, Peng WC, Gros P, Clevers H. The R-spondin/Lgr5/Rnf43 module: regulator of Wnt signal strength. Gene Dev. 2014;28(4):305–16.
10. Tsai JH, Liau JY, Yuan CT, Cheng ML, Yuan RH, Jeng YM. RNF43 mutation frequently occurs with GNAS mutation and mucin hypersecretion in intraductal papillary neoplasms of the bile duct. Histopathology. 2017;70(5):756–65.
11. Koo BK, Spit M, Jordens I, Low TY, Stange DE, van de Wetering M, van Es JH, Mohammed S, Heck AJ, Maurice MM, et al. Tumour suppressor RNF43 is a stem-cell E3 ligase that induces endocytosis of Wnt receptors. Nature. 2012;488(7413):665–9.
12. Min BH, Hwang J, Kim NKD, Park G, Kang SY, Ahn S, Ahn S, Ha SY, Lee YK, Kushima R, et al. Dysregulated Wnt signalling and recurrent mutations of the tumour suppressor RNF43 in early gastric carcinogenesis. J Pathol. 2016;240(3):304–14.
13. Yoon K, Lee S, Han TS, Moon SY, Yun SM, Kong SH, Jho S, Choe J, Yu J, Lee HJ, et al. Comprehensive genome- and transcriptome-wide analyses of mutations associated with microsatellite instability in Korean gastric cancers. Genome Res. 2013;23(7):1109–17.
14. Lee YS, Cho YS, Lee GK, Lee S, Kim YW, Jho S, Kim HM, Hong SH, Hwang JA, Kim SY, et al. Genomic profile analysis of diffuse-type gastric cancers. Genome Biol. 2014;15(4):,R55.

15. Loregger A, Grandl M, Mejias-Luque R, Allgauer M, Degenhart K, Haselmann V, Oikonomou C, Hatzis P, Janssen KP, Nitsche U, et al. The E3 ligase RNF43 inhibits Wnt signaling downstream of mutated beta-catenin by sequestering TCF4 to the nuclear membrane. *Sci Signal* 2015, 8(393).
16. Wei CY, Zhang X, He S, Liu BL, Han HF, Sun XJ. MicroRNA-219-5p inhibits the proliferation, migration, and invasion of epithelial ovarian cancer cells by targeting the Twist/Wnt/beta-catenin signaling pathway. Gene. 2017;637:25–32.
17. Liu L, Zhang YX, Cao WK. Highly expressed lncRNA LOC730101 promotes lung cancer cell growth through Wnt canonical pathway. *Biochem Bioph Res Co* 2017, 493(2),992–997.
18. Murillo-Garzon V, Kypta R. WNT signalling in prostate cancer. Nat Rev Urol. 2017;14(11):683–96.
19. Debebe A, Medina V, Chen CY, Mahajan IM, Jia C, Fu D, He L, Zeng N, Stiles BW, Chen CL, et al. Wnt/beta-catenin activation and macrophage induction during liver cancer development following steatosis. Oncogene. 2017;36(43):6020–9.
20. Cho SG. APC downregulated 1 inhibits breast cancer cell invasion by inhibiting the canonical WNT signaling pathway. Oncol Lett. 2017;14(4):4845–52.
21. Song Y, Li ZX, Liu X, Wang R, Li LW, Zhang QY. The Wnt/beta-catenin and PI3K/Akt signaling pathways promote EMT in gastric cancer by epigenetic regulation via H3 lysine 27 acetylation. *Tumor Biol* 2017, 39(7).
22. Huang L, Wu RL, Xu AM. Epithelial-mesenchymal transition in gastric cancer. Am J Transl Res. 2015;7(11):2141–58.
23. Christiansen JJ, Rajasekaran AK. Reassessing epithelial to mesenchymal transition as a prerequisite for carcinoma invasion and metastasis. Cancer Res. 2006;66(17):8319–26.
24. Ryland GL, Hunter SM, Doyle MA, Rowley SM, Christie M, Allan PE, Bowtell DD, Australian Ovarian Cancer Study G, Gorringe KL, Campbell IG. RNF43 is a tumour suppressor gene mutated in mucinous tumours of the ovary. J Pathol. 2013;229(3):469–76.
25. Zou Y, Wang F, Liu FY, Huang MZ, Li W, Yuan XQ, Huang OP, He M. RNF43 mutations are recurrent in Chinese patients with mucinous ovarian carcinoma but absent in other subtypes of ovarian cancer. Gene. 2013;531(1):112–6.
26. Jiang X, Hao HX, Growney JD, Woolfenden S, Bottiglio C, Ng N, Lu B, Hsieh MH, Bagdasarian L, Meyer R, et al. Inactivating mutations of RNF43 confer Wnt dependency in pancreatic ductal adenocarcinoma. Proc Natl Acad Sci U S A. 2013;110(31):12649–54.
27. Niu L, Qin HZ, Xi HQ, Wei B, Xia SY, Chen L. RNF43 Inhibits Cancer Cell Proliferation and Could be a Potential Prognostic Factor for Human Gastric Carcinoma. Cell Physiol Biochem. 2015;36(5):1835–46.
28. Lechner M, Boshoff C, Beck S. Cancer epigenome. Adv Genet. 2010;70:247–76.
29. Janjigian YY, Azzoli CG, Krug LM, Pereira LK, Rizvi NA, Pietanza MC, Kris MG, Ginsberg MS, Pao W, Miller VA, et al. Phase I/II trial of cetuximab and erlotinib in patients with lung adenocarcinoma and acquired resistance to erlotinib. Clin Cancer Res. 2011;17(8):2521–7.

30. Yi JH, Heo SJ, Lee CK, Jung M, Kim HS, Chung HC, Rha SY. A salvage treatment with combination of docetaxel and epiruhicin in patients with recurrent or metastatic gastric cancer after fluoropyrimidine failure. *J Clin Oncol* 2014, 32(15).
31. Cavanna L, Bodini FC, Stroppa EM, Banchini F, Michieletti E, Capelli P, Zangrandi A, Anselmi E. Advanced Gastric Cancer with Liver and Lymph Node Metastases Successfully Resected after Induction Chemotherapy with Docetaxel, Cisplatin and 5-Fluorouracil. Chemotherapy. 2014;60(4):224–7.
32. Janjigian YY, Shah MA. Molecularly targeted therapies in advanced gastric cancer. Minerva Gastroenterol Dietol. 2011;57(1):75–88.
33. To KKW, Poon DC, Wei YM, Wang F, Lin G, Fu LW. Pelitinib (EKB-569) targets the up-regulation of ABCB1 and ABCG2 induced by hyperthermia to eradicate lung cancer. Brit J Pharmacol. 2015;172(16):4089–106.
34. Hegedus C, Truta-Feles K, Antalffy G, Varady G, Nemet K, Ozvegy-Laczka C, Keri G, Orfi L, Szakacs G, Settleman J, et al. Interaction of the EGFR inhibitors gefitinib, vandetanib, pelitinib and neratinib with the ABCG2 multidrug transporter: implications for the emergence and reversal of cancer drug resistance. Biochem Pharmacol. 2012;84(3):260–7.
35. Aravindan N, Aravindan S, Herman TS, Natarajan MEGFR. Tyrosine Kinase Inhibitor Pelitinib Regulates Radiation-Induced p65-Dependent Telomerase Activation in Squamous Cell Carcinoma. Radiat Res. 2013;179(3):304–12.
36. Janjigian YY, Park BJ, Zakowski MF, Ladanyi M, Pao W, D'Angelo SP, Kris MG, Shen R, Zheng J, Azzoli CG. Impact on disease-free survival of adjuvant erlotinib or gefitinib in patients with resected lung adenocarcinomas that harbor EGFR mutations. J Thorac Oncol. 2011;6(3):569–75.
37. Gungor H, Saleem A, Babar S, Dina R, El-Bahrawy MA, Curry E, Rama N, Chen M, Pickford E, Agarwal R, et al. Dose-Finding Quantitative 18F-FDG PET Imaging Study with the Oral Pan-AKT Inhibitor GSK2141795 in Patients with Gynecologic Malignancies. J Nucl Med. 2015;56(12):1828–35.
38. Algazi AP, Esteve-Puig R, Nosrati A, Hinds B, Hobbs-Muthukumar A, Nandoskar P, Ortiz-Urda S, Chapman PB, Daud A. Dual MEK/AKT inhibition with trametinib and GSK2141795 does not yield clinical benefit in metastatic NRAS-mutant and wild-type melanoma. *Pigment Cell Melanoma Res* 2017.
39. Dumble M, Crouthamel MC, Zhang SY, Schaber M, Levy D, Robell K, Liu Q, Figueroa DJ, Minthorn EA, Seefeld MA, et al. Discovery of novel AKT inhibitors with enhanced anti-tumor effects in combination with the MEK inhibitor. Plos One. 2014;9(6):,e100880.
40. Maurer U, Preiss F, Brauns-Schubert P, Schlicher L, Charvet C. GSK-3-at the crossroads of cell death and survival. J Cell Sci. 2014;127(7):1369–78.

Tables

Table 1. Association of RNF43 and PWWP2B expression with clinicopathological characteristics in 34 gastric cancer patients.

Characteristics	RNF43 low/PWWP2B low FC[1]<2.0 (%)	RNF43 high/PWWP2B lowFC[1]>2.0 (%)	*P*-value
Age	69.0 (44-87)	62.5 (61-64)	
Sex			
Male	17(50.0)	2(5.9)	
Female	15(44.1)	0	
Tumor location			
Pylorus	1 (2.9)	0	1.000
Antrum	20 (58.8)	2 (5.9)	<0.001
Body	6 (17.7)	0	0.025
Pylorus ~ Antrum	1 (2.9)	0	1.000
Antrum ~ Body	4 (11.8)	0	0.114
Lauren's classification			
Diffuse	15 (44.1)	0	<0.001
Intestinal	6 (17.7)	1 (2.9)	0.105
Mixed	11 (32.4)	1 (2.9)	0.003
Cancer stage, TNM class			
I	1 (2.9)	0	1.000
II	9 (26.5)	0	0.027
III	22 (64.7)	0	<0.001
IV	0	2 (5.9)	0.493
Recurrence	11/11(100)	0	<0.001

[1]FC, fold change.

Table 2. IC_{50} of selected drugs in HAP1, HAP1 RNF43 KO and HAP1 PWWP2B KO cells.

Drug	HAP-1	PWWP2B	RNF43
	IC_{50} (uM)		
Aprepitant	17.25	14.89	16.25
Docetaxel Trihydrate (nM)	19.83	19.31	17.19
Ethinyl Estradiol	18.85	15.88	16.42
Griseofulvin	16.00	13.46	15.56
INC280	39.13	37.56	28.08
Pelitinib	3.14	2.03	0.71
Pimobendan	13.23	11.81	12.38
Tepotinib	23.17	21.38	19.07
Uprosertib	4.93	3.02	2.99

Additional File

Additional file 1 RNF43 and PWWP2B gene expression as measured by quantitative real-time PCR in cancer cell lines.

Figures

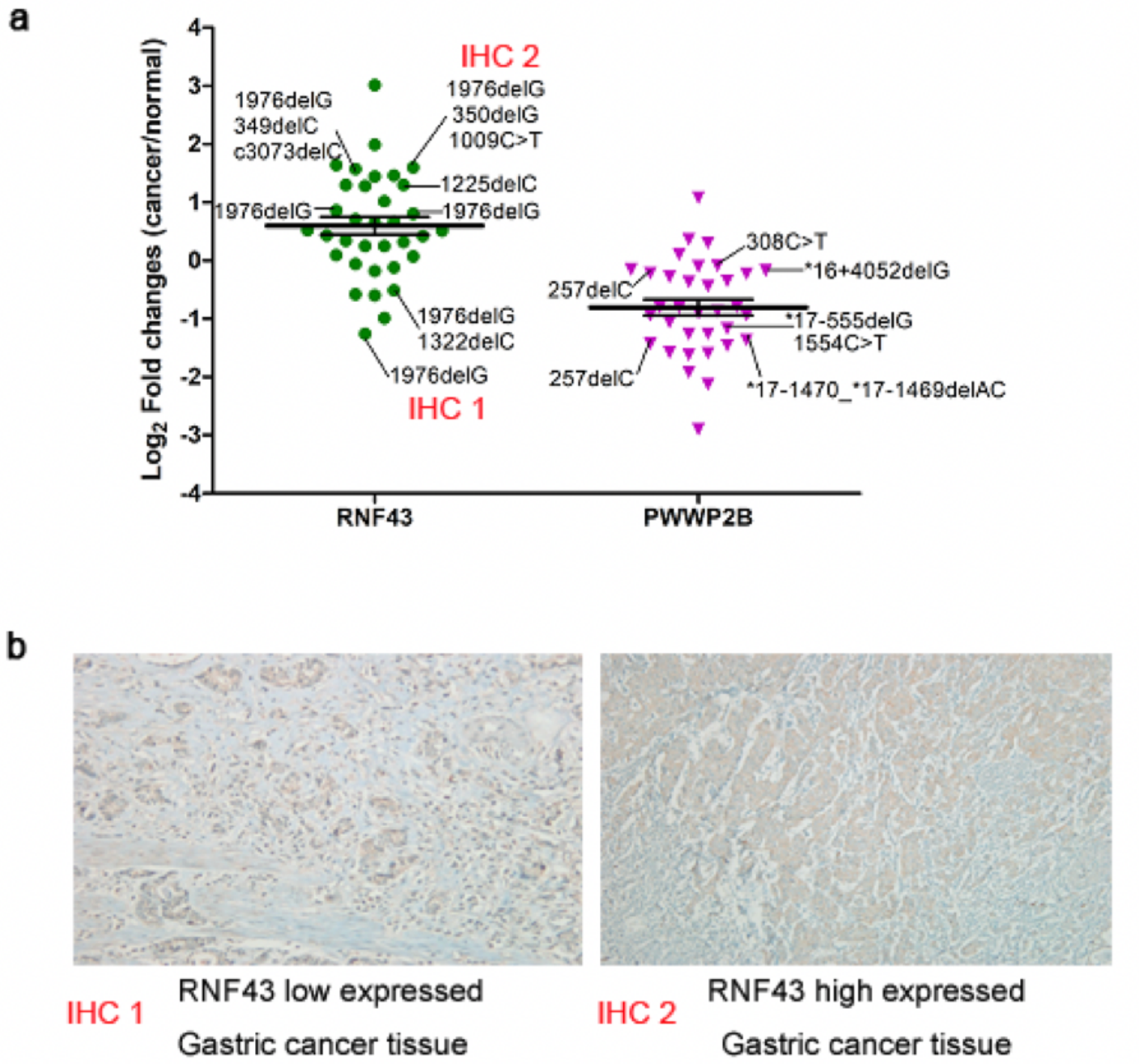

Figure 1

Expression analysis of RNF43 and PWWP2B in gastric cancer and adjacent normal tissues. a mRNA expression of RNF43 and PWWP2B genes in 34 gastric cancer patients. Gastric cancer patients harboring RNF43 or PWWP2B mutation. b Immunohistochemical analysis of RNF43 in low or high RNF43 mRNA expressed gastric cancer tissues (x 200).

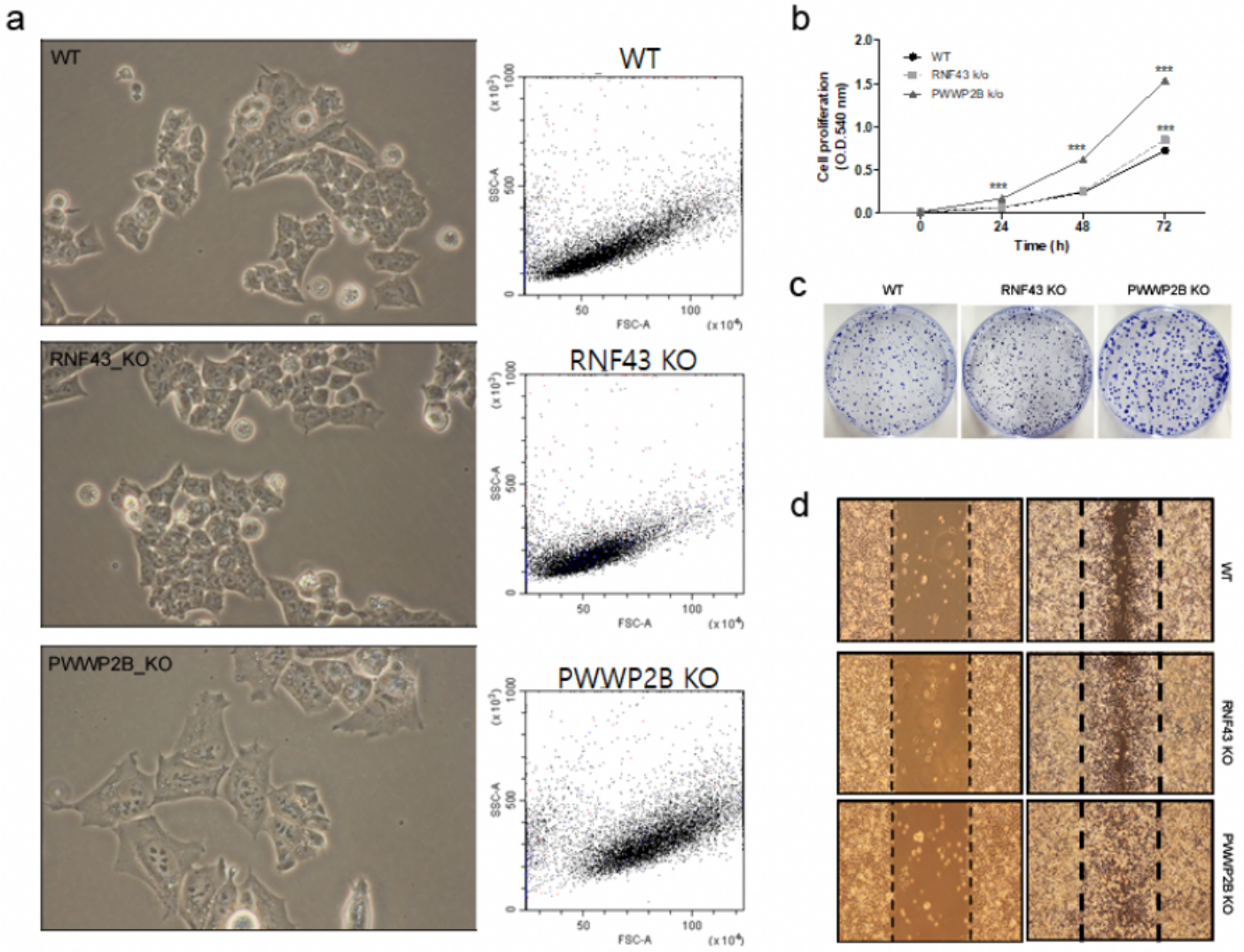

Figure 2

Characterization of RNF43 KO and PWWP2B KO cells. a Representative images (left column) and cell size (middle column) of RNF43KO and PWWP2B cells (x400). b The MTT cell proliferation assay was performed after 0, 24, 48, and 72 h. Data represent the mean value of three experiments performed in triplicate. c The effects of RNF43 and PWWP2B KO on cell proliferation were evaluated by crystal violet staining. d The wound-healing assay was used to assess the effects of RNF43 and PWWP2B KO on the migration ability of HAP1 cells. Both RNF43 KO and PWWP2B KO cells showed increased migration ability compared with control cell lines. WT, wild type; KO, knockout; *** $P < 0.001$ compared with the WT.

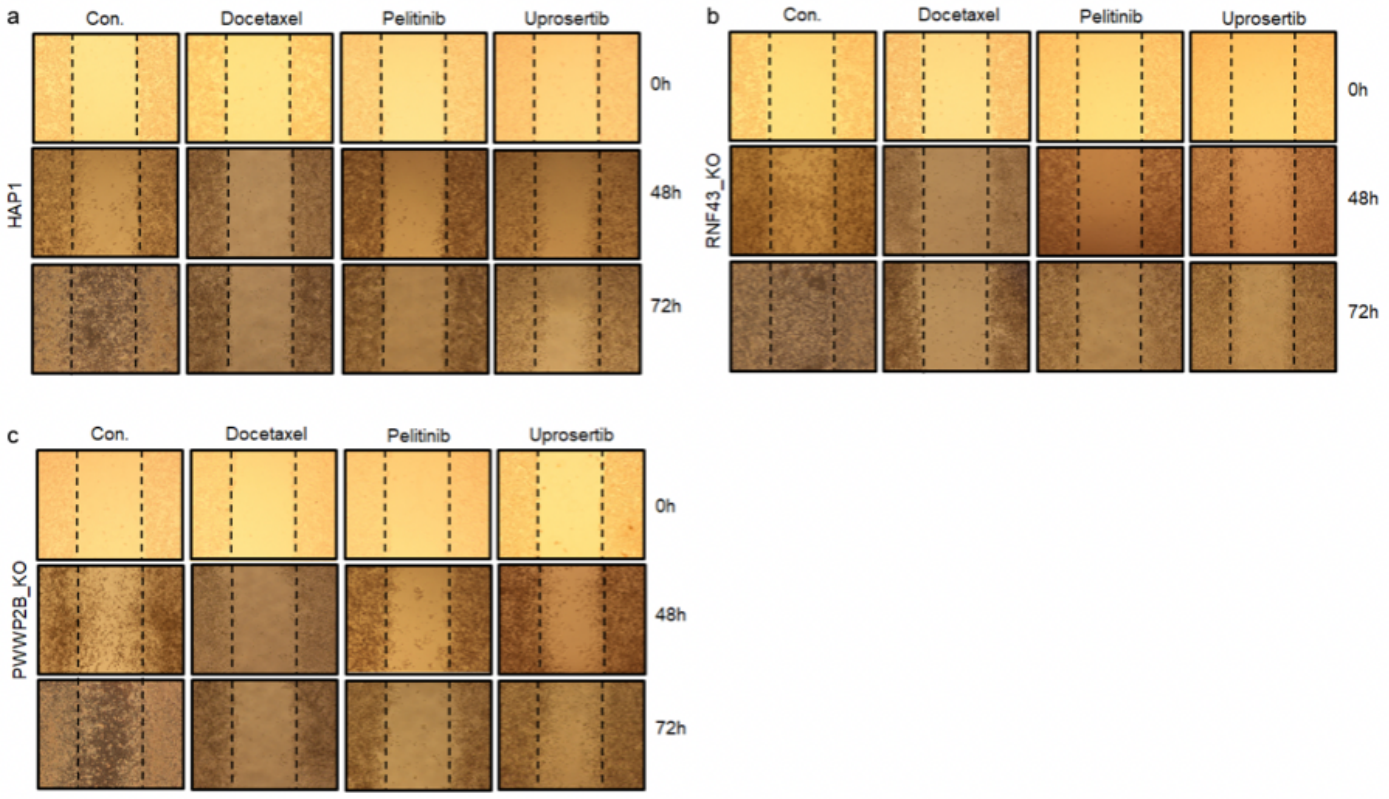

Figure 3

Anti-migration activities of docetaxel, pelitinib, and uprosertib in HAP1, HAP1 RNF43 KO, and HAP1 PWWP2B KO cells. The wound-healing assay of (a) HAP1, (b) HAP1 RNF43 KO, and (c) HAP1 PWWP2B KO cells treated with the respective half maximal inhibitory concentration (IC50) values of docetaxel trihydrate, pelitinib or uprosertib. Docetaxel trihydrate-, pelitinib- and uprosertib-treated cells showed inhibited migration ability compared with control cell lines. Con, control; KO, knockout.

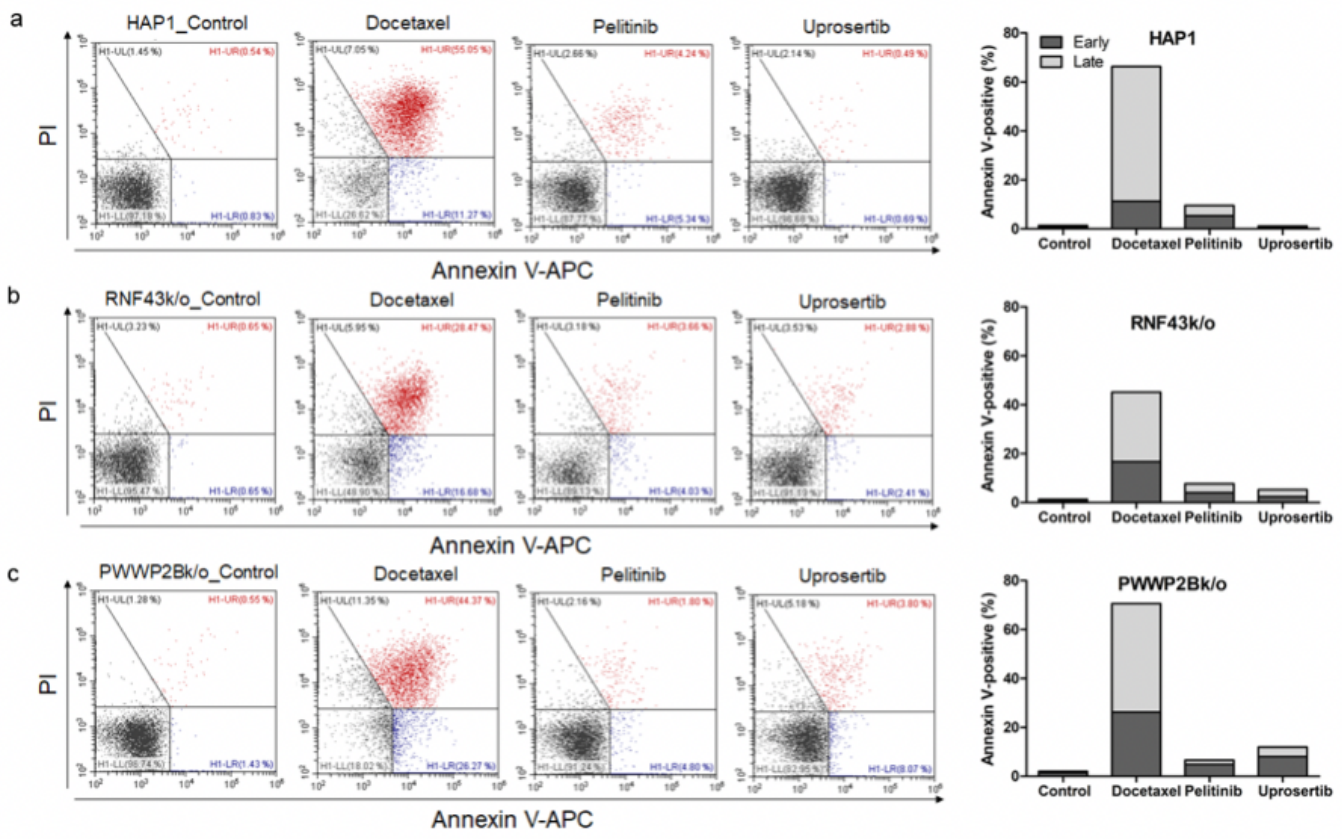

Figure 4

Apoptotic activities of docetaxel, pelitinib, and uprosertib in HAP1, HAP1 RNF43 KO, and HAP1 PWWP2B KO cells. Flow cytometric assay of (a) HAP1, (b) HAP1 RNF43 KO, and (c) HAP1 PWWP2B KO cells treated with the respective half maximal inhibitory concentration (IC50) values of docetaxel trihydrate, pelitinib or uprosertib. Docetaxel trihydrate-, pelitinib- and uprosertib-treated cells showed induced apoptosis ability compared with control cell lines. PI, propidium iodide; Con, control; KO, knockout.

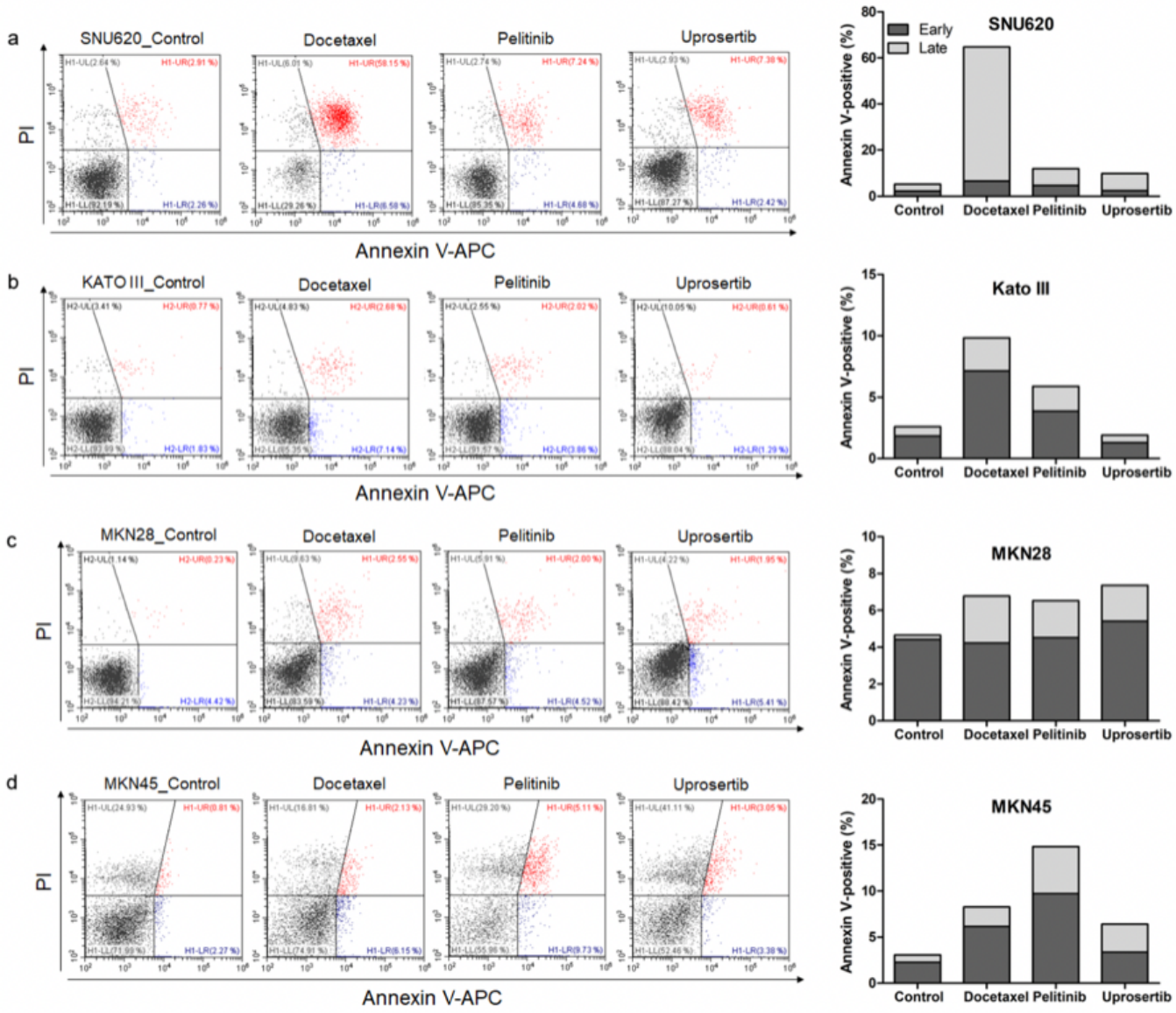

Figure 5

Apoptotic activities of docetaxel, pelitinib, and uprosertib in gastric cancer cell lines established from metastasis to the peritoneal cavity (Kato III and SNU620 cells) and gastric carcinoma cell lines (MKN28 and MKN45). Flow cytometric assay of (a) SNU620, (b) Kato III, (c) MKN28, and (d) MKN45 cells treated with 12nM, 5uM, and 5uM concentration values of docetaxel trihydrate, pelitinib or uprosertib. Docetaxel trihydrate-, pelitinib- and uprosertib-treated cells showed induced apoptosis ability compared with control cell lines. PI, propidium iodide; Con, control; KO, knockout.

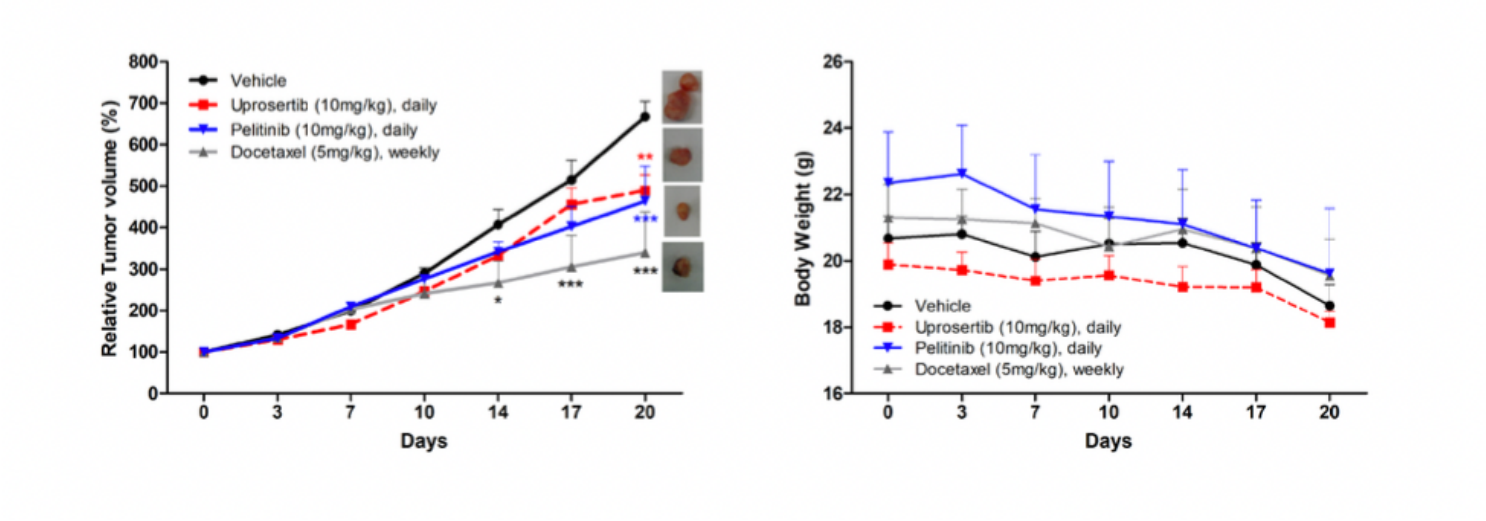

Figure 6

Anti-tumor growth activities of docetaxel, pelitinib, and uprosertib in vivo. The effects of relative tumor volume and body weight of MKN45 xenograft mouse treatmented with docetaxel trihydrate (5mg/kg/weekly, intraperitoneally), pelitinib (10mg/kg/day, oral gavage) or uprosertib (10mg/kg/day, oral gavage) at described concentrations. All error bars are s.e.m. * $P < 0.05$, ** $P < 0.01$, and *** $P < 0.001$ compared with control (vehicle) group.

Supplementary Files

This is a list of supplementary files associated with this preprint. Click to download.

- Additionalfile1.doc